

Controlling the Morphology of Zinc Oxide Nanorods Crystallized from Aqueous Solutions: The Effect of Crystal Growth Modifiers on Aspect Ratio

Simon P. Garcia^{*,†} and Steve Semancik

Chemical Science and Technology Laboratory, National Institute of Standards and Technology,
Gaithersburg, Maryland 20899

Received August 22, 2006. Revised Manuscript Received May 25, 2007

The effect of growth modifiers on the morphology of zinc oxide (ZnO) nanorods crystallized from solution is characterized. During hydrolysis of zinc nitrate at pH = 7.6 and 75 °C, hexagonally prismatic ZnO crystals were grown in the presence of three growth modifiers: poly(diallyldimethylammonium chloride) (PDADMAC), sodium poly(styrene sulfonate) (PSS), and trisodium citrate. Using statistical analyses of scanning electron microscopy (SEM) images, crystal dimensions were quantified, and the median aspect ratio (ratio of prism length to width) was determined as a function of modifier concentration. In the absence of growth modifiers, the median crystal aspect ratio was 5.2. The aspect ratio was reduced to 4.7, 2.5, and 0.25 in the presence of, respectively, 67 nmol/L (nM) PDADMAC, 130 nM PSS, and 40 μ mol/L (μ M) citrate. These effects are explained in terms of both electrostatic and coordinative binding between growth modifier and crystal surface.

Introduction

The control of crystal shape is an important challenge in the synthesis and assembly of microcrystalline and nanocrystalline materials. Shape control is especially desirable for inorganic semiconductors because their electronic and optical properties can be strongly influenced by the size and morphology of constituent crystals. In nanocrystalline ZnO films, for example, using elongated, rod-like ZnO crystals instead of spherical crystals increases the overall electron mobility by a factor of 50.¹ This approach could potentially improve the efficiency of photoelectrochemical devices based on ZnO² and on other inorganic materials.³ In addition, the incorporation of high-aspect-ratio nanocrystals into porous films could help increase the sensitivity of conductometric sensing devices.⁴

Solution-based processes provide attractive routes for synthesizing structured ZnO materials. Many are based on the hydrolysis of zinc salts in aqueous solution to generate hydroxozincate complexes and the subsequent condensation of these complexes into ZnO. Through these methods, a wide variety of crystal shapes are possible, including spheres, ellipsoids, tapered needles, untapered rods, and thin, plate-like membranes.^{5–8} Unfortunately, crystal morphology can

depend sensitively on several reaction parameters, including temperature,^{5,9} pH,^{10,11} time of growth,¹² seed crystals,^{13,14} and impurities.⁷

Sensitivity to growth conditions can be overcome by using substances known as growth modifiers. When added to the crystallizing solution, growth modifiers alter the shape of crystals as they grow, thus providing *chemical* control of crystal morphology. Despite this potential, the chemical basis of growth modification is still not completely understood, especially for metal oxide materials. Why do some modifiers lead to spherical crystals, while others lead to elongated, rod-like crystals, and still others have no effect at all? How are these effects mediated by temperature and pH? Can these effects be correlated with differences in the growth modifier's molecular structure? With a more complete understanding of growth modifier chemistry, modifiers could be chosen or designed rationally for desirable ZnO morphologies. In addition, growth modification could also be used to control the morphology of ZnO films grown on substrates. Processes that produce structured films using low-pH, low-temperature growth conditions are becoming increasingly valuable in the development of solid-state devices that incorporate ZnO.^{15–17}

[†] Present address: Department of Chemistry, Kenyon College, Gambier, Ohio 43022.

- (1) Sun, B.; Siringhaus, H. *Nano Lett.* **2005**, *5*, 2408.
- (2) Baxter, J. B.; Aydii, E. S. *Appl. Phys. Lett.* **2005**, *86*, 53114.
- (3) Huynh, W. U.; Dittmer, J. J.; Alivisatos, A. P. *Science* **2002**, *295*, 2425.
- (4) Jiaqiang, X.; Yuping, C.; Daoyong, C.; Jianian, S. *Sens. Actuators, B* **2006**, *113*, 526.
- (5) Chittofrati, A.; Matijevic, E. *Colloids Surf.* **1990**, *48*, 65.
- (6) Andrés Vergés, M.; Mifsud, A.; Serna, C. J. *J. Chem. Soc., Faraday Trans.* **1990**, *86*, 959.
- (7) Li, P.; Wei, Y.; Liu, H.; Wang, X.-K. *J. Solid State Chem.* **2005**, *178*, 855.

- (8) Trindade, T.; Pedrosa de Jesus, J. D.; O'Brien, P. J. *Mater. Chem.* **1994**, *4*, 1611.
- (9) Dem'yanets, L. N.; Kostomarov, D. V.; Kuz'mina, I. P. *Inorg. Mater.* **2002**, *38*, 124.
- (10) Kawano, T.; Imai, H. *Cryst. Growth Des.* **2006**, *6*, 1054.
- (11) Oliveira, A. P. A.; Hocheplid, J.-F.; Grillon, F.; Berger, M.-H. *Chem. Mater.* **2003**, *15*, 3202.
- (12) McBride, R. A.; Kelly, J. M.; McCormack, D. E. *J. Mater. Chem.* **2003**, *13*, 1196.
- (13) Li, Q.; Kumar, V.; Li, Y.; Zhang, H.; Marks, T. J.; Chang, R. P. H. *Chem. Mater.* **2005**, *17*, 1001.
- (14) Pauporté, Th.; Cortés, R.; Froment, M.; Beaumont, B.; Lincot, D. *Chem. Mater.* **2002**, *14*, 4702.
- (15) Vayssieres, L.; Keis, K.; Hagfeldt, A.; Lindquist, S.-E. *Chem. Mater.* **2001**, *13*, 4395.

How do growth modifiers affect crystal morphology? Growth modification is usually explained in terms of anisotropic, *face-specific* growth kinetics. Because crystal faces are chemically distinct, each face grows at a different rate, and these differences determine the shape of the crystal as it grows. Through face-specific reactions with crystal surfaces, growth modifiers can alter the relative growth rates of each face and thus effect changes in crystal shape. Investigations of growth modification in ZnO crystallization have revealed a number of trends in the chemistry of growth modification. Small anions, such as counterions from the zinc salt (e.g., nitrate, chloride, acetate, sulfate), have only subtle effects on crystal shape.^{6,18} Alkali metal cations are similarly ineffective as growth modifiers (with the exception of Li⁺).¹⁹ In contrast, species with *multiple coordination sites*, such as chelating agents (e.g., EDTA²⁰ and triethanolamine^{5,21,22}) and polyelectrolytes,^{23–26} can have dramatic effects on morphology. Valency is not the sole factor controlling crystal morphology, however. For example, solution pH sometimes mediates a growth modifier's effects; in some cases, changing the pH can even reverse these effects.²⁰ To investigate the roles of charge and coordinative valency in growth modification, we characterize the effects of three potential growth modifiers on the crystallization of ZnO nanorods from aqueous solution: sodium poly(styrene sulfonate) (PSS), poly(diallyldimethylammonium chloride) (PDADMAC), and trisodium citrate. PSS and PDADMAC are polyelectrolytes containing multiple (10²–10³) charged functional groups on each molecule. PSS contains sulfonate groups, which remain completely ionized in aqueous solutions and are negatively charged. PDADMAC contains tertiary amine groups, which remain completely ionized in aqueous solutions and are positively charged. In contrast, citrate is a small molecule with three carboxylate groups. At the pH of our system, citrate is completely deprotonated and has three negatively charged sites. In this manuscript, we observe and quantify the dimensions and shapes of crystals produced with different concentrations of each modifier. We identify morphological changes and correlate them with modifier concentration. With this set of modifiers, we compare the morphological effects of charge (positively charged PSS against negatively charged PDADMAC) and of valency (citrate with 3 coordination sites against PSS with ~370 sites).

Experimental Section

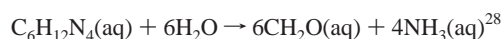
The products of crystal growth are often highly sensitive to the initial nucleation process. To control for this sensitivity, seed crystals

Table 1. Growth Modifier Concentrations

PDADMAC	PSS	citrate
0 nM	0 nM	0 μ M
7 nM	13 nM	10 μ M
67 nM	130 nM	20 μ M
		40 μ M

of ZnO were prepared separately according to a procedure adapted from Haase et al.²⁷ Stock solutions of NaOH in methanol (0.20 M) and zinc nitrate hexahydrate in methanol (0.20 M) were dispersed by agitation in a low-power, ultrasonic bath for 10 min. From these stock solutions, a solution of tetrahydroxozincate was prepared by diluting 4 mL of the NaOH stock solution with 196 mL of methanol and adding 1.0 mL of the zinc nitrate stock solution under vigorous stirring. In a separate solution, 1.4 mL of the zinc nitrate stock solution and 1.0 mL of H₂O were added to 20 mL of methanol. This solution was added dropwise to the tetrahydroxozincate solution, which became opalescent. The resulting ZnO sol was stirred at 19 °C for 18 h and then diluted with 200 mL of methanol.

ZnO nanorods were grown from these seed crystals by the hydrolysis and condensation of Zn(II) ions in aqueous solution. In each experiment, 8 mL of an aqueous growth solution, containing zinc nitrate hexahydrate (10 mM) and methenamine (C₆H₁₂N₄; 10 mM), were prepared in a glass vial. A total of 200 μ L of the ZnO sol described above was added to provide seed crystals. To study the effects of growth modifiers, 5–200 μ L of solutions containing sodium PSS (average $M_w \sim 77\,400$, Fluka), PDADMAC (average $M_w \sim 150\,000$, Sigma-Aldrich), or trisodium citrate (Sigma-Aldrich) was added. Table 1 lists the growth modifier concentrations, on the basis of molar ratio, that were tested. At the initial pH of 6.0, this system is undersaturated with respect to ZnO crystallization. To initiate crystal growth, the vial was tightly capped and immersed in a 75 °C water bath. At this temperature, methenamine decomposes to formaldehyde and ammonia:



The resulting in situ production of NH₃ shifts the pH to 7.6 and effects supersaturation, as evidenced by opacity of the growth solution after 15 min. After 2.5 h at 75 °C, crystals were isolated by vacuum filtration of the suspension through a track-etched, polycarbonate membrane (pore size = 100 nm, Whatman Nucleopore). The crystals were washed four times with deionized water, washed twice with absolute ethanol, and stored under ethanol.

The sizes and morphologies of the resulting crystals were characterized by scanning electron microscopy (SEM). To prepare a sample for imaging, a batch of crystals was dispersed in 1.0 mL of ethanol, using a 20-W ultrasonic horn with 30 1.0-s pulses for a total of 30 s. A 5- μ L drop of this suspension was placed on a 5 × 5 mm piece of bare silicon and allowed to evaporate in air (about 20 s). For each film prepared in this way, at least 16 unique images were obtained from different points on the sample.

Results and Discussion

In the absence of growth modifiers, aqueous crystal growth of ZnO results in elongated, rod-like crystals. Using X-ray diffraction, we confirmed that the product was crystalline

- (16) Wang, Z.; Qian, X.-F.; Yin, J.; Zhu, Z.-K. *Langmuir* **2004**, *20*, 3441.
- (17) Tian, Z. R.; Voigt, J. A.; Liu, J.; McKenzie, B.; McDermott, M. J.; Rodriguez, M. A.; Konishi, H.; Zu, H. *Nat. Mater.* **2003**, *2*, 821.
- (18) Yamabi, S.; Imai, H. *J. Mater. Chem.* **2002**, *12*, 3773.
- (19) Uekawa, N.; Yamashita, R.; Wu, Y. J.; Kakegawa, K. *Phys. Chem. Chem. Phys.* **2004**, *6*, 442.
- (20) DiLeo, L.; Romano, D.; Schaeffer, L.; Gersten, B.; Foster, C.; Gelabert, M. C. *J. Cryst. Growth* **2004**, *271*, 65.
- (21) Chen, D.; Jiao, X.; Cheng, G. *Solid State Commun.* **2000**, *113*, 363.
- (22) Govender, K.; Boyle, D. S.; Kenway, P. B.; O'Brien, P. *J. Mater. Chem.* **2004**, *14*, 2575.
- (23) Zhang, H.; Yang, D.; Li, D.; Ma, X.; Li, S.; Que, D. *Cryst. Growth Des.* **2005**, *5*, 547.
- (24) Taubert, A.; Palms, D.; Weiss, Ö.; Piccini, M.-T.; Batchelder, D. N. *Chem. Mater.* **2002**, *14*, 2394.

- (25) Öner, M.; Norwig, J.; Meyer, W. H.; Wegner, G. *Chem. Mater.* **1998**, *10*, 460.
- (26) Kumar, R. V.; Elgamiel, R.; Koltypin, Y.; Norwig, J.; Gedanken, A. *J. Cryst. Growth* **2003**, *250*, 409.
- (27) Haase, M.; Weller, H.; Henglein, A. *J. Phys. Chem.* **1988**, *92*, 482.

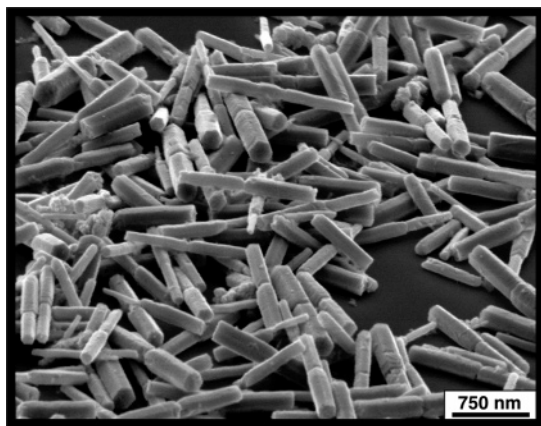


Figure 1. SEM image of ZnO crystals grown by hydrolysis, in the absence of growth modifier. Crystals are prismatic with a hexagonal cross section.

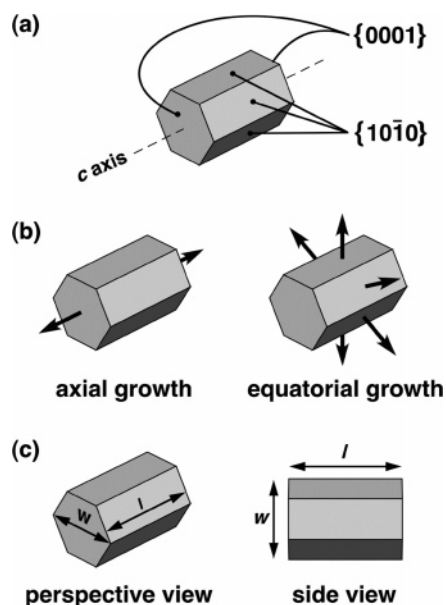


Figure 2. Primary growth faces on hexagonally prismatic crystals with wurtzite structure. (a) Hexagonal faces are parallel to $\{0001\}$ lattice planes, whereas lateral prism faces are parallel to $\{10\bar{1}0\}$ lattice planes. (b) Axial growth is normal to hexagonal faces, and equatorial growth is normal to lateral prism faces. (c) Two dimensions specify crystal shape: width w across the hexagonal face and length l across the lateral faces.

ZnO of the zincite phase. From the SEM image in Figure 1, we can make a few qualitative observations about crystal size and shape. The crystals are prismatic with hexagonal cross sections. The cross section's sixfold symmetry is consistent with the wurtzite lattice structure of this phase. These highly symmetrical crystals have two types of surfaces: the $\{0001\}$ and $\{10\bar{1}0\}$ prism faces, which are illustrated in Figure 2. Crystals are typically shorter than 1 μm and narrower than 250 nm. Prismatic crystals have also been observed in other ZnO growth processes, at a variety of temperatures and pH.^{5–8,12,20,23}

The vast majority of crystals appear to be twinned. We have found that this effect depends strongly on the presence of seed crystals, because growth in the absence of seed crystals yields both twinned crystals and spherulitic clusters of prismatic crystals (not shown). Indeed, twinning and spherulitic aggregation are observed under a wide variety of growth conditions.^{5,6,29} Because previous investigators have observed twinning early in the growth process,⁶ we

suspect that the appearance of these crystals is not due to the aggregation of prismatic crystals after growth.

The elongated form of these crystals is the result of growth anisotropy between different crystal faces. The hexagonally prismatic shape of ZnO crystals suggests two principal types of face-specific growth, illustrated in Figure 2b: *axial growth*, which is normal to the $\{0001\}$ lattice planes and directed along the c -axis of symmetry, and *equatorial growth*, which is normal to the $\{10\bar{1}0\}$ planes and directed radially from the c -axis. Differences between axial and equatorial growth affect one important parameter of crystal shape: aspect ratio, which is the ratio of a crystal's *length* (its extension along the sixfold axis of symmetry) and its *width* (the distance between opposite corners on the hexagonal cross section). Aspect ratios therefore provide a first clue for inferring the relative reactivity of different crystal faces. For example, the high aspect ratio of an elongated crystal implies that axial growth is significantly faster than equatorial growth.

All of the crystals grown in this study took the form of hexagonal prisms: any differences were in the aspect ratio. Other investigators using this growth process have reported that aspect ratio is time-independent after 30 min,⁶ so after 2.5 h, we observe the steady-state crystal morphology. For this reason, the aspect ratio of a crystal provides a measure of the ratio of axial growth to equatorial growth.

Quantifying Crystal Morphology. To compare growth processes, the resulting crystals' aspect ratios must be measured and characterized statistically. Two parameters can be determined by direct inspection of SEM images: crystal width w and crystal length l . Figure 2c illustrates these dimensions for a hexagonally prismatic crystal. The width is defined as the distance between opposite corners across the hexagonal face, while the length is defined as its extension normal to this face. When viewed from the side (90° off-axis), such a crystal should appear as a rectangle, and both width and length can be measured. From these measurements aspect ratios can be calculated.

The morphology of a real crystal, however, often deviates from the form of a perfectly hexagonal prism. For example, many crystals exhibit some tapering along their c -axes, so that one end is narrower than the other and the side profile is trapezoidal instead of rectangular. This effect leaves the definition of crystal width somewhat ambiguous: should the width at the wider end or the narrower end be recorded? To resolve this ambiguity, we fit a rectangle to the polygon defined by each crystal's profile. For each crystal (twinned crystals were treated as two separate particles), points are drawn upon the image to outline a crystal's boundaries, and the rectangle fit to these points is a function whose only parameters are length and width. The best-fit values of these parameters are taken as the dimensions of the crystal. Using this method, the length and width of more than 300 crystals were measured for each set of the growth conditions considered in this study.

The greatest source of uncertainty in these measurements arises in determining each crystal's boundary. The actual

(28) Tada, H. *J. Am. Chem. Soc.* **1960**, 82, 255.

(29) Ma, X.; Zhang, H.; Ji, Y.; Xu, J.; Yang, D. *Mater. Lett.* **2005**, 59, 3393.

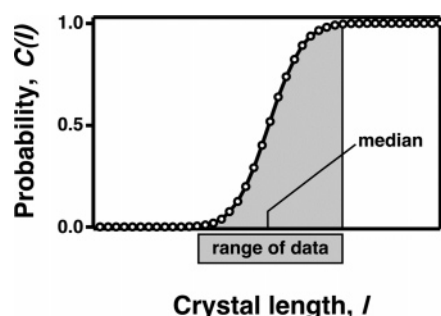


Figure 3. Hypothetical cumulative distribution function for normally distributed data (e.g., crystal length l). $C(l)$ increases rapidly over the range of the data, giving rise to a characteristic “shoulder”. The median value of l is defined by $C(l) = 0.5$.

position of a point on the boundary may lie anywhere between two adjacent pixels. Given the image resolution of 13.9 nm/pixel, we assume that errors in the measured position are uniformly distributed within an interval of 13.9 nm. We therefore estimate the uncertainty in width and length at 16 nm (assuming a coverage factor of $k = 2$). The corresponding uncertainty in aspect ratio depends on crystal size. Because we are primarily interested in comparing median values, we estimate this uncertainty for each growth condition on the basis of median values of crystal length and width; typical values for aspect ratio uncertainty range from 8% to 12% of the aspect ratio.

From these measurements, the distributions of crystal length, width, and aspect ratio were calculated. To describe these data, we use *cumulative* probability distributions instead of the more familiar probability distribution, because cumulative distributions facilitate comparison among distributions with similar modes but widely varying widths. For a given property, such as crystal length l , the probability distribution $P(l)$ gives the probability density for crystals of length l . In contrast, the corresponding cumulative distribution $C(l)$ gives the probability that a crystal's length is *smaller* than l . Figure 3 illustrates a hypothetical cumulative distribution for normally distributed data. A cumulative distribution $C(l)$ increases monotonically from 0 to 1, primarily in a “shoulder” that extends over a band of l values. This shoulder is centered on the median value, l_{med} , which is defined by $C(l_{\text{med}}) = 0.5$. As illustrated in Figure 3, the band indicates the range of the data. In comparing distributions, two features of $C(l)$ are important: the position of this band, which corresponds to the median of the data, and its width, which indicates the variability of this data. If a change in growth process produced shorter crystals, for example, the shoulder in the cumulative distribution would shift toward smaller values of l . Similarly, a narrow band (indicated by a steep shoulder) would indicate a high degree of uniformity in crystal length, whereas a wide band (gradually sloping shoulder) would indicate highly variable lengths among crystals.

Absence of Growth Modifier (Control). Figure 4a shows sample ZnO crystals grown in the absence of growth modifiers. The corresponding distributions of aspect ratios and crystal lengths are indicated by the “0 nM” lines graphed in Figure 5a,b. The aspect ratios are consistently greater than 1 and range from 3 to 10. The crystal length distribution is

centered at $l \sim 1030$ nm and ranges from 500 to 1200 nm. Although the distribution appears to have a small shoulder at $l \sim 550$ nm, this feature may reflect limited counting statistics, rather than a genuinely bimodal distribution. Median values of each crystal dimension are listed in Table 2. With a median aspect ratio of 5.2, these crystals have essentially the same shape as those produced by other investigators using the same growth chemistry; however, the previous studies have reported much larger crystals (length $> 2 \mu\text{m}$).^{6,8} This discrepancy might be explained by the use of seed crystals, which allow a higher density of crystallization centers and thus lead to smaller particle size. The presence of seed crystals should have no effect, however, on face-specific growth rates or on aspect ratio.

Effect of PDADMAC. Figure 4 compares crystals grown at 0 nM (unmodified), 7 nM, and 67 nM of PDADMAC. The presence of PDADMAC in the growth solution seems to have no dramatic effect on crystal shape. In all cases, crystals are hexagonally prismatic and elongated along the c -axis. The aspect ratio distribution, shown in Figure 5a, is only subtly affected, with the median aspect ratio decreasing by only $\sim 10\%$. The crystal length distribution displayed in Figure 5b, however, is affected by PDADMAC in two ways. First, the median crystal length is reduced from 1029 to 713 nm, a decrease of nearly 30%. Second, the length of PDADMAC-modified crystals is more uniform, as evidenced by the sharpness of the shoulder in the cumulative distribution. Interestingly, a 10-fold increase in concentration (from 7 nM to 67 nM) has virtually no effect on these distributions.

Effect of PSS. The presence of PSS in the growth solution has a number of effects on crystal morphology. As shown in Figure 6, crystals retain hexagonally prismatic forms in all cases. Increasing the PSS concentration leads to a visible reduction in both crystal length and aspect ratio. This trend is quantified in the aspect ratio and crystal length distributions displayed in Figure 7a,b. As the PSS concentration is increased, each distribution shifts to progressively lower values. By 130 nM of PSS, the median crystal length is reduced by more than 50% from 1029 to 463 nm, while the median aspect ratio is similarly reduced from 5.2 to 2.5. Interestingly, PSS modification also leads to crystals with rough surfaces. This effect is most obvious for 130 nM PSS, where each crystal's sidewalls exhibit a scalloped appearance.

The concentration-dependent reduction in aspect ratio implies that PSS alters the growth anisotropy, either by decelerating axial growth or by accelerating equatorial growth.³⁰ These two situations cannot be distinguished, however, without absolute measurements of growth rate for each face. Although the exact chemical mechanism of ZnO growth at near-neutral pH has not been fully explained, growth modification usually involves face-specific adsorption of the modifier to the crystal surfaces. Adsorbed species can suppress growth on a surface by “blocking” the attachment of growth units until they are displaced or are buried by the next atomic layer.³¹ In an alternative explanation, adsorbed species could *enhance* surface growth by reducing electro-

(30) Cabrera, N.; Vermilyea, D. A. In *Growth and Perfection of Crystals*; Doremus, R. H., Roberts, B. W., Turnbull, D., Eds.; Wiley: New York, 1958; p 393.

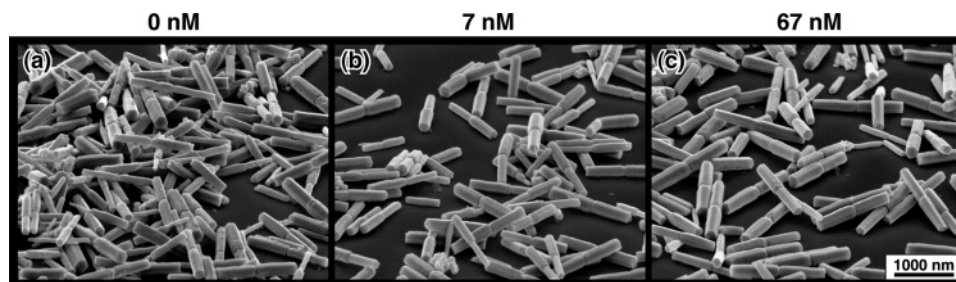


Figure 4. ZnO crystals grown in the presence of (a) 0 nM (control), (b) 7 nM, and (c) 67 nM of PDADMAC. Crystals are hexagonally prismatic in all cases.

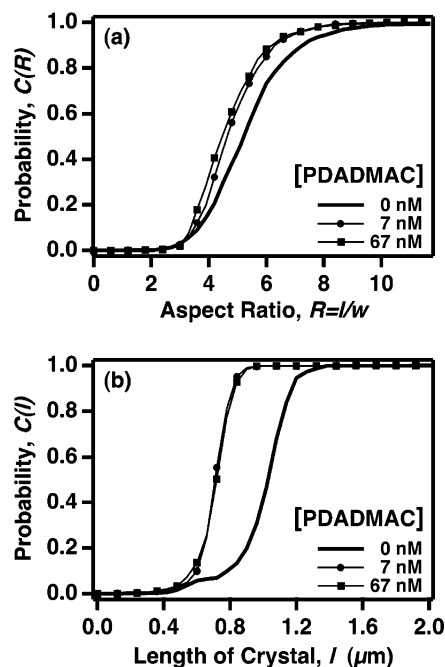


Figure 5. Cumulative distributions of (a) aspect ratio R and of (b) crystal length l for ZnO crystals grown in the presence of PDADMAC.

Table 2. Median Aspect Ratios and Lengths for PDADMAC and PSS

growth modifier and concentration	aspect ratio, R	length, l (nm)
no modifier	5.2 ± 0.4	1029 ± 16
PDADMAC, 7 nM	4.7 ± 0.5	713 ± 16
PDADMAC, 67 nM	4.5 ± 0.5	719 ± 16
PSS, 13 nM	4.0 ± 0.5	574 ± 16
PSS, 130 nM	2.5 ± 0.2	463 ± 16

static repulsion between a charged surface and like-charged growth units.³²

Table 2 compares the aspect ratio and length for different concentrations of PSS and PDADMAC. Why does PSS have such a strong, concentration-dependent effect on crystal morphology, whereas PDADMAC does not? These differences could be explained by considering electrostatic interactions between the crystal surface and growth modifier. Because the point of zero charge (pzc) for ZnO is 9.0,³³ each crystal in a pH = 7.6 solution develops a positive charge on its surfaces. This charge should lead to significant adsorption of anionic species, such as PSS, which is ionized in aqueous

solutions and carries negatively charged coordination sites. If the surface charge density depends on the crystal face, then PSS adsorption would be promoted on crystal faces with greater surface charge density. Assuming that the adsorbed species inhibits or enhances growth, changes in growth rate would be face-specific. Positively charged PDADMAC, in contrast, would adsorb only minimally, if at all, on positively charged crystal surfaces. As a result, PDADMAC would not significantly affect the growth anisotropy.

If face-specific charge is the basis of anisotropic growth, then why do small anions, such as chloride, sulfate, and acetate, have little or no effect on aspect ratio, especially when compared to a polymeric anion such as PSS? These species do not affect crystal shape to the extent that 130 nM of PSS does, even at concentrations greater than 10^5 ppb.^{6,18} PSS's effectiveness at changing aspect ratio may be due to its multivalent nature: each molecule provides multiple (on average, ~ 370) sites for binding with the crystal surface. Because these sites are connected, removal of one site from the surface requires the collective displacement of its many neighboring sites, which is a highly improbable event. As a result, minute concentrations of PSS are sufficient to alter the growth chemistry of crystal faces.

Effect of Citrate. Figure 8 shows that citrate has a dramatic effect on ZnO growth morphology. As citrate concentration is increased from 10 μM to 40 μM , the crystals' cross sections become progressively larger while their lengths decrease. This trend leads to thin, plate-like, hexagonal crystals, and when the citrate concentration is 20 μM or greater, the crystals are *wider* than they are long. These observations are illustrated quantitatively by the distributions in Figure 9 and the values in Table 3. First, the aspect ratio distribution shifts to progressively lower values as citrate concentration increases, with the median aspect ratio decreasing to 0.25 with 40 μM of citrate. Second, the width of the distribution is markedly reduced at higher citrate concentrations. With 10 μM citrate, the aspect ratio distribution ranges from 0.5 to 5.0, but for 20 μM and 40 μM citrate, the aspect ratios are narrowly distributed. Growth modification by citrate also seems to result in crystals with larger cross sections. This effect is illustrated by the crystal *width* distributions, $C(w)$, shown in Figure 9b. With increasing citrate concentration, the crystal width distribution shifts to progressively larger widths. Like PSS, citrate does not affect the twinning of crystals.

As with PSS, the reduction (and eventual inversion) of growth anisotropy implies either axial growth inhibition or equatorial growth acceleration. The marked decrease in

(31) Frank, F. C. In *Growth and Perfection of Crystals*; Doremus, R. H., Roberts, B. W., Turnbull, D., Eds.; Wiley: New York, 1958; p 411.

(32) Mullin, J. W. *Crystallization*; Butterworths: Oxford, 1993; Chapter 6.

(33) Parks, G. A. *Chem. Rev.* **1965**, 65, 177.

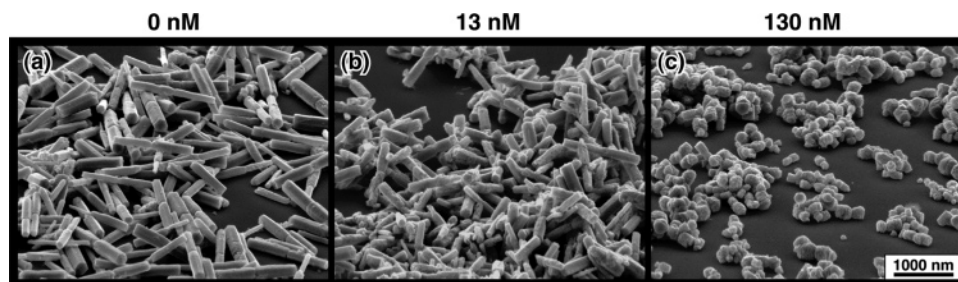


Figure 6. ZnO crystals grown in the presence of (a) 0 nM (control), (b) 13 nM, and (c) 130 nM of PSS.

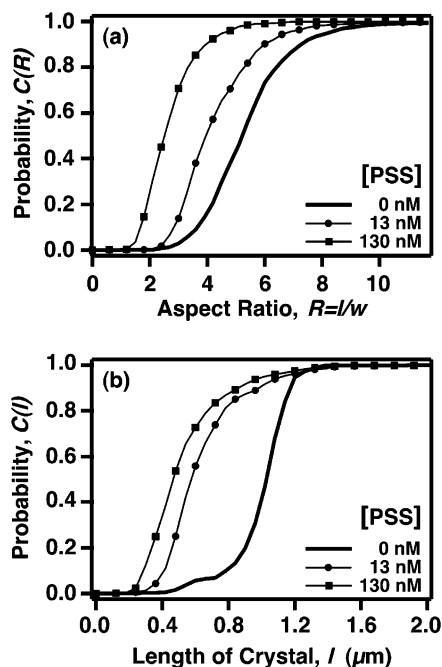


Figure 7. Cumulative distributions of (a) aspect ratio R and of (b) crystal length l for ZnO crystals grown in the presence of PSS.

crystal length with increasing citrate concentration would imply that citrate inhibits axial growth; however, the increase in crystal width could imply that citrate accelerates equatorial growth. We cannot conclude, however, that citrate has the opposite effects on each face. It is possible that citrate suppresses nucleation, which would allow higher supersaturation in the solution and therefore larger crystal dimensions overall. In either case, absolute growth rate measurements will be necessary to understand citrate's effects more completely.

How does PSS compare with citrate in terms of growth anisotropy? If aspect ratio is controlled by a growth modifier's coordinative valency, then molecules with more binding sites should be more effective in changing aspect ratio. On this basis, PSS, which carries approximately 370 anionic functional groups on each molecule, should cause more dramatic morphological changes compared to citrate, which has only three anionic sites. If we consider the range of concentrations needed to change aspect ratio, then PSS appears to follow this prediction. The concentration range required for modifying the aspect ratio by citrate is more than 100 times the concentration range required for modification by PSS. This type of comparison, however, overlooks the *change* in aspect ratio due to a given change in concentration. Citrate is remarkably effective in altering the anisotropy of crystal growth. With citrate, the median aspect

ratio can be reduced by 40–70% simply by doubling citrate concentration (e.g., 10 to 20 μM or 20 to 40 μM). Obtaining the same effect with PSS requires a *factor-of-10* increase in PSS concentration. The number of coordination sites is therefore not the only factor that determines the growth anisotropy.

The striking effect of citrate may be due to the spatial orientation of its three carboxylate groups. Because the relative positions of these moieties enjoy little flexibility (compared to a polymer), coordinative binding with the crystal surface may be highly sensitive to the surface's molecular structure, which is face-specific. We tentatively hypothesize that citrate binds strongly with $\{0001\}$ crystal faces (which possess threefold rotational symmetry) but weakly with $\{10\bar{1}0\}$ faces (which do not) and that axial growth is therefore drastically suppressed (through a blocking process) compared to equatorial growth. In contrast, PSS binding to crystal faces is likely to be insensitive to surface structure; in this case, only surface charge density provides a basis for face-specific binding.

Citrate may have roles in growth modification beyond adsorbing to crystal surfaces. In solution, citrate binds Zn^{2+} ions as a chelating ligand and reduces the availability of Zn^{2+} for deposition on crystal surfaces. At 40 μM , citrate binding is expected to increase the solubility of ZnO by a factor of 3,³⁴ thus decreasing supersaturation. This effect would clearly decrease the absolute rate of crystal growth, but its effect on face-specific growth is unclear. If citrate-bound $\text{Zn}(\text{II})$ complexes can somehow deposit Zn^{2+} ions directly on crystal surfaces, thus behaving as additional growth units, then any mechanism of citrate-mediated growth habit modification would have to consider the face-specific reactivity of this species.

How would the binding of citrate lead to the observed changes in aspect ratio? We can approach this question by considering the reactivity of defect sites, including steps and kinks, on a crystal face. Anisotropic growth is likely to be dominated by the attachment of atoms to these sites. On a crystal face, for example, growth would depend on two sequential processes: the formation of atomic-height steps (either by two-dimensional nucleation or by screw dislocations),³⁵ and the subsequent motion of these steps as atoms attach to the step edges. Taken together, these two processes result in the addition of new layers to a crystal face and thus control growth normal to that face.

(34) Kragten, J. *Atlas of Metal-Ligand Equilibria in Aqueous Solutions*; Ellis Horwood: Chichester, 1978; Chapter 45.

(35) Burton, W. K.; Cabrera, N.; Frank, F. C. *Philos. Trans. R. Soc.* **1951**, A243, 299.

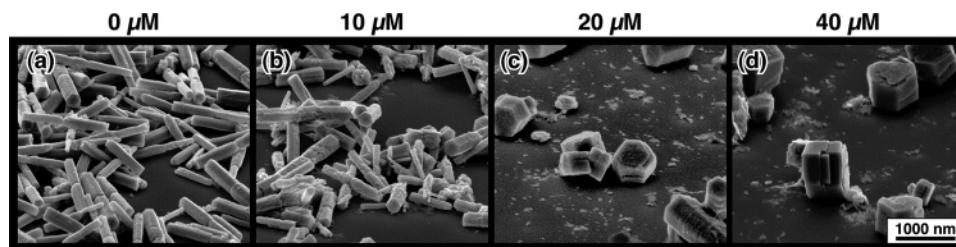


Figure 8. ZnO crystals grown in the presence of (a) 0 μM (control), (b) 10 μM , (c) 20 μM , and (d) 40 μM of citrate.

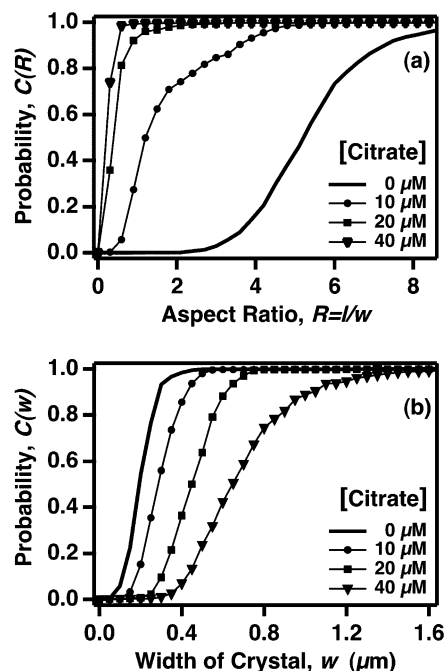


Figure 9. Cumulative distributions of (a) aspect ratio R and of (b) crystal width w for ZnO crystals grown in the presence of citrate.

Table 3. Median Aspect Ratios and Widths for Citrate

citrate concentration (μM)	aspect ratio, R	width, w (nm)
0 (no modifier)	5.2 ± 0.4	190 ± 16
10	1.2 ± 0.1	284 ± 16
20	0.35 ± 0.04	450 ± 16
40	0.25 ± 0.03	645 ± 16

Assuming that growth on the hexagonal face proceeds through such a mechanism, citrate can effect changes in aspect ratio by mediating either process. For example, citrate could bind to steps at the terrace edges and prevent growth along these steps. This effect, known as “step pinning,” has been observed in the citrate-modified growth of calcium oxalate monohydrate³⁶ and would lead to a macroscopically rough crystal face. Alternatively, citrate might bind preferentially to flat terrace sites and inhibit two-dimensional nucleation,

which would favor growth at step edges and encourage the formation of flat surfaces. Our qualitative observations of crystal surface morphology indicate that the hexagonal face of most crystals (grown with and without modifiers) is smooth, suggesting that citrate does not prefer steps on the hexagonal face. A systematic characterization of surface morphology would be helpful to probe the effects of growth modification in two ways. First, the mechanism by which steps are produced would be evident in the surface morphology following growth: either growth spirals or layers would be observed. Second, the effects of a growth modifier on surface growth would be observed as specific features, such as step pinning or changes in the density of nucleated layers.

Conclusions

The morphological effects of three growth modifiers on the crystal growth of hexagonally prismatic ZnO nanorods have been quantified. PDADMAC, a cationic polyelectrolyte, produces negligible effects on crystal shape. PSS and citrate, both anionic, significantly reduce the aspect ratio of crystals. Comparison of PSS with PDADMAC suggests that face-specific surface charge density plays a role in growth modification. The dramatic effects of citrate, however, imply that coordinative binding also provides a basis for chemically altering growth anisotropy.

Acknowledgment. We thank Kurt Benkstein and Christopher Montgomery for their advice and assistance with the preparation of seed crystals. We are also grateful to Albert Davydov for X-ray diffraction analysis and to James Kelly and Mark Vaudin for their advice on crystal characterization. S.P.G. acknowledges the support of the National Research Council Postdoctoral Research Associateship Program at the National Institute of Standards and Technology.

CM061977R

(36) Qiu, S. R.; Wierzbicki, T. A.; Orme, C. A.; Cody, A. M.; Hoyer, J. R.; Nancollas, G. H.; Zepeda, S.; de Yoreo, J. J. *Proc. Natl. Acad. Sci. U.S.A.* **2004**, *101*, 1811.